

Neutron Reflectivity and Atomic Force Microscopy Studies of a Lipid Bilayer in Water Adsorbed to the Surface of a Silicon Single Crystal

B. W. Koenig,[†] S. Krueger,[‡] W. J. Orts,[‡] C. F. Majkrzak,[‡] N. F. Berk,[‡]
J. V. Silverton,[†] and K. Gawrisch^{*,§}

Laboratory of Biophysical Chemistry, NHLBI, NIH, Bethesda, Maryland 20892-1676,
Materials Science and Engineering Laboratory, NIST, Gaithersburg, Maryland 20899-0001,
and Laboratory of Membrane Biochemistry and Biophysics, NIAAA, NIH,
12501 Washington Avenue, Rockville, Maryland 20852

Received July 14, 1995. In Final Form: November 20, 1995[®]

Specular reflection of neutrons has been used to characterize the structure of single lipid bilayers adsorbed to a planar silicon surface from aqueous solution. We used a novel experimental setup which significantly decreased the incoherent background scattering and allowed us to measure neutron reflectivities as low as 5×10^{-7} . Thicknesses and neutron scattering length densities were determined by a fitting procedure using (i) randomly generated smooth functions represented by parametric B-splines and (ii) stepped functions based on the theoretical lipid composition. The size of lipid domains at the surface and the degree of surface coverage were determined by atomic force microscopy. Chain-protonated and -deuterated dipalmitoylphosphatidylcholine (DPPC) bilayers were investigated in $^2\text{H}_2\text{O}$ and a mixture of $^2\text{H}_2\text{O}$ and H_2O which matches the scattering density of silicon. Also, one measurement on a distearoylphosphatidylcholine bilayer which has longer acyl chains was performed for comparison. The lipid adsorbs to the silicon surface as a continuous layer interrupted by irregularly shaped uncovered areas which are 100–500 Å in size. The surface coverage was estimated to be $70 \pm 20\%$. The reflectivity measurements on DPPC at 60 °C show a silicon oxide layer with a thickness of the order of 4 Å, a rough silicon oxide/water layer between silicon oxide and lipid with a thickness between 2 and 8 Å, and a single lipid bilayer. Fitting resolved a central membrane layer with a thickness of 28 ± 2 Å which represents the lipid hydrocarbon chains. This layer is sandwiched between interface membrane layers of lipid head groups and water which are 11.5 ± 1 Å in thickness. The angstrom-scale thickness changes of the central membrane layer as a function of the phase state of the lipid and of the length of the hydrocarbon chains are easily detected.

Introduction

Single lipid bilayers in water are a very useful model system for studying physical and functional properties of biological membranes. Single lipid bilayers can be investigated as unilamellar vesicles, as black lipid membranes (BLM) formed in a small window between two water chambers, or as bilayers adsorbed to the surface of a solid substrate. BLM's have been widely used to study transport phenomena across model membranes, the influence of lipid–protein interaction on membrane structure, and membrane fusion.¹ However, BLM's are difficult to investigate using methods which provide direct structural information. X-ray and neutron studies on unilamellar vesicles have been attempted.^{2,3} Here we investigate the geometry of single lipid bilayers adsorbed to the surface of silicon single crystals using specular reflection of neutrons and atomic force microscopy (AFM).

While specular reflection of neutrons is sensitive to the neutron scattering length density distribution along the normal to the bilayer surface,⁴ AFM provides information about the lateral organization of lipids at the surface.^{5–8} Both methods require the bilayer to be supported by an

atomically smooth, solid interface and allow the membrane to be investigated in an aqueous environment.

Supported single lipid bilayers (SSLB) can be manufactured by a sophisticated Langmuir–Blodgett film deposition procedure,⁹ by spontaneous fusion of small unilamellar lipid vesicles to the solid/water interface,¹⁰ or by a combination of both methods (monolayer fusion technique).^{11,12} Either quartz or single-crystalline silicon serves as solid substrate of the bilayer in neutron reflectivity measurements. In spite of the strong coupling of the lower leaflet of the lipid membrane with the underlying substrate (presumably due to electrostatic interactions between the lipid head groups and the SiO_2 groups of the surface⁹ and van der Waals attraction), basic physical features of the membrane were not influenced in SSLB's. The lateral diffusion behavior of several phosphatidylcholine lipids was observed to be virtually identical to that in multilamellar systems.⁹ The transition temperatures between different lamellar phases were reported to be only slightly lower for SSLB's than for uni- or multilamellar lipid vesicles.^{9,13} However, the presence of the solid substrate prevents the formation of the ripple

* To whom correspondence should be addressed.

[†] NIH, Bethesda.

[‡] NIST.

[§] NIH, Rockville.

[®] Abstract published in *Advance ACS Abstracts*, February 15, 1996.

(1) Hanke, W.; Schlue, W.-R. *Planar lipid bilayers. Methods and applications*; Academic Press Limited: London, 1993.

(2) Lewis, B. A.; Engelman, D. M. *J. Mol. Biol.* **1983**, *166*, 211.

(3) Sadler, D. M.; Reiss-Husson, F.; Rivas, E. *Chem. Phys. Lipids*. **1990**, *52*, 41.

(4) Johnson, S. J.; Bayerl, T. M.; McDermott, D. C.; Adam, G. W.; Rennie, A. R.; Thomas, R. K.; Sackmann, E. *Biophys. J.* **1991**, *59*, 289.

(5) Yang, J.; Tamm, L. K.; Somlyo, A. P.; Shao, Z. *J. Microsc.* **1993**, *171*, 183.

(6) Hui, S. W.; Viswanathan, R.; Zasadzinski, J. A.; Israelachvili, J. N. *Biophys. J.* **1995**, *68*, 171.

(7) Mou, J.; Yang, J.; Huang, C.; Shao, Z. *Biochemistry* **1994**, *33*, 9981.

(8) Mou, J.; Yang, J.; Shao, Z. *J. Mol. Biol.* **1995**, *248*, 507.

(9) Tamm, L. K.; McConnell, H. M. *Biophys. J.* **1985**, *47*, 105.

(10) Brian, A. A.; McConnell, H. M. *Proc. Natl. Acad. Sci. U.S.A.* **1984**, *81*, 6159.

(11) Fringeli, U. P. In *Biologically Active Molecules: Identification, Characterization, and Synthesis: Proceedings of a Seminar on Chemistry of Biologically Active Compounds, Interlaken, September 5–7, 1988*; Schlunegger, U. P., Ed.; Springer-Verlag: Berlin, 1989; p 241.

(12) Kalb, E.; Frey, S.; Tamm, L. K. *Biochim. Biophys. Acta* **1992**, *1103*, 307.

phase (P_β) between the low-temperature gel phase (L_β or $L_{\beta'}$) and the liquid-crystalline phase (L_α).^{4,13} The feasibility of the reconstitution of membrane protein into SSLB's¹⁰ and the binding of monoclonal antibodies to SSLB's¹⁴ has been demonstrated.

Penfold and Thomas have reviewed the application of specular reflection of neutrons to the study of surfaces and interfaces.¹⁵ The technique has successfully been used to study the structure of monolayers of surfactants^{16,17} as well as of lipids^{18,19} at the air/liquid interface. The method is also suited to structural investigations of surfactant bilayers adsorbed to a solid support in an aqueous environment.^{20–24} In papers by Johnson et al.⁴ and Reini et al.,²⁵ specular reflection of neutrons has been used to obtain structural information of lipid bilayers. A first attempt to characterize the structure of a protein, streptavidine, bound to a solid supported lipid monolayer by means of neutron reflectivity has been published.²⁶

The aim of the present study was to characterize the structure of lipid bilayers which adsorb spontaneously to the surface of silicon wafers from sonicated lipid–water dispersions. We used a novel experimental setup²⁷ which allows measurement of neutron reflectivity over a wider range of momentum transfer than in any of the previous studies. The data were interpreted by fitting the profile of stepped functions or of randomly generated smooth functions to the experimental data of two lipids with hydrocarbon chains of a differing length. Lateral organization of lipids was studied by atomic force microscopy in order to aid the interpretation of the neutron reflectivity curves. The results allow us to estimate the thickness of the adsorbed lipid bilayer, the SiO_2 layer, and the water layer between them.

Materials and methods⁴⁰

Neutron Reflectometry Measurements. Specular reflection of neutrons was measured at the fixed-wavelength ($\lambda = 2.367$ Å) reflectometer BT-7 at the National Institute of Standards and Technology in Gaithersburg, MD.²⁸ Data were acquired in the θ – 2θ mode with incident angles θ between 0 and 3.3° using a ^3He detector. The accessed range of the momentum transfer perpendicular to the sample surface ($Q = 4\pi \sin \theta / \lambda$) was $0 < Q \leq 0.3 \text{ Å}^{-1}$. A double-slit geometry provided a narrow primary beam having a horizontal divergence of approximately 1 min of arc.

The sample cell (Figure 1) consists of a trough ($110 \times 65 \times 30 \text{ mm}^3$) carved into a Teflon block. One side-wall of the trough

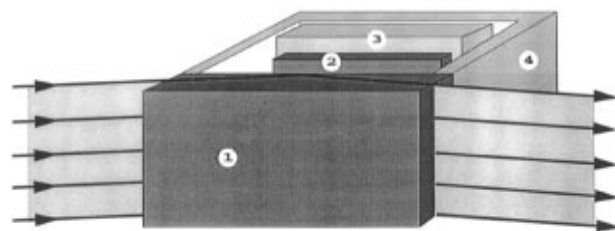


Figure 1. Drawing of the sample cell. A large stationary silicon block (1) seals the water-filled Teflon container (4) via an O-ring (not shown). A smaller silicon block (2) is set into a Teflon frame (3), and the assembly can be moved to adjust the distance between both blocks. The incident neutron beam passes through the large silicon block before getting partially reflected on striking the silicon/water interfaces. The specular reflected intensity is directed toward the detector (not shown).

was removed, and the chamber was sealed with a viton O-ring against a stationary single-crystal silicon block ($152 \times 76 \times 25 \text{ mm}^3$). A second, movable single-crystal silicon block ($102 \times 51 \times 12 \text{ mm}^3$) was mounted inside the cell using a Teflon frame. The surfaces of the two blocks which are facing each other have been polished by the manufacturer (Semiconductor Processing, Inc., Boston, MA) to provide atomically smooth substrates for lipid adsorption. The cell was filled either with $^2\text{H}_2\text{O}$ or a mixture of H_2O and $^2\text{H}_2\text{O}$ having the same neutron scattering length density as silicon and is referred to as silicon-matched water (SMW). The water-filled gap between the two blocks can easily be adjusted from the centimeter down to the micrometer range by moving the smaller silicon block. Thus, the distance between blocks can be kept in the micrometer range during the measurements but adjusted to the centimeter range for sample manipulations such as addition of lipid or protein, the exchange of solvent, etc.

The incident neutron beam enters the large silicon block through the end face and is specularly reflected on striking the silicon/water interfaces at glancing angle. The reflected beam emerges through the opposite end face of the same block. The attenuation of the neutron beam on passing through silicon is comparatively weak. The transmission of 2.367 Å neutrons is about 75% for a single-crystal silicon block of 152 mm length. The entire side of the sample cell facing the detector except for the end face of the large silicon block was covered with a strong neutron absorber (boron-enriched rubber). This was done to prevent background intensity arising from additional scattering of the neutron beam by parts of the sample cell.

Bilayer Preparation. 1,2-Dipalmitoyl-*sn*-glycero-3-phosphocholine (DPPC), 1,2-distearoyl-*sn*-glycero-3-phosphocholine (DSPC), and DPPC with perdeuterated acyl chains (DPPC- d_{62}) were purchased from Avanti Polar Lipids (Birmingham, AL). Small unilamellar vesicles (SUV's) were obtained by sonication for 5 min of 30 mg of lipid in 5 mL of deionized water at a temperature slightly above the main phase transition of the lipid.

The silicon blocks were cleaned first in detergent solution and then placed in concentrated H_2SO_4 containing NOCHROMIX (Godax Laboratories, Inc., New York, NY) for 30 min. The Teflon parts and the O-ring were soaked in soap solution, rinsed, and finally boiled in deionized water to remove the detergent. After the silicon blocks were rinsed carefully with deionized water the cell was assembled under water. The water-filled cell was enclosed in an aluminum cell holder. The temperature of the silicon blocks was adjusted to a value 10°C above the main phase transition of the lipid by controlling the temperature of the cell holder with a water bath circulator. The SUV dispersion was added to the temperature-adjusted sample cell resulting in a final lipid concentration of 0.5 mg/mL. The cell content was thoroughly mixed. The lipid vesicles were allowed to diffuse and adsorb to the silicon surfaces over a period of 1 h. Afterward the sample cell was rinsed once with deionized water at the elevated temperature to remove excess lipid. Finally, the water in the sample cell was exchanged three times for $^2\text{H}_2\text{O}$ or SMW, respectively, below the main phase transition temperature of the lipid.

Data Treatment. The reflectivity is the ratio of the intensity of the reflected beam to that of a beam transmitted through the length of the large silicon block without reflection. The reflectivity curves were corrected for background, slit opening size, and finite

(13) Naumann, C.; Brumm, T.; Bayerl, T. M. *Biophys. J.* **1992**, *63*, 1314.

(14) Tamm, L. K. *Biochemistry* **1988**, *27*, 1450.

(15) Penfold, J.; Thomas, R. K. *J. Phys.: Condens. Matter* **1990**, *2*, 1369.

(16) Simister, E. A.; Lee, E. M.; Thomas, R. K.; Penfold, J. *J. Phys. Chem.* **1992**, *96*, 1373.

(17) Lu, J. R.; Li, Z. X.; Su, T. J.; Thomas, R. K.; Penfold, J. *Langmuir* **1993**, *9*, 2408.

(18) Bayerl, T. M.; Thomas, R. K.; Penfold, J.; Rennie, A. R.; Sackmann, E. *Biophys. J.* **1990**, *57*, 1095.

(19) Vaknin, D.; Kjaer, K.; Als-Nielsen, J.; Lösche, M. *Biophys. J.* **1991**, *59*, 1325.

(20) Lee, E. M.; Thomas, R. K.; Cummins, P. G.; Staples, E. J.; Penfold, J.; Rennie, A. R. *Chem. Phys. Lett.* **1989**, *162*, 196.

(21) Rennie, A. R.; Lee, E. M.; Simister, E. A.; Thomas, R. K. *Langmuir* **1990**, *6*, 1031.

(22) McDermott, D. C.; Lu, J. R.; Lee, E. M.; Thomas, R. K.; Rennie, A. R. *Langmuir* **1992**, *8*, 1204.

(23) McDermott, D. C.; Kanelleas, D.; Thomas, R. K.; Rennie, A. R.; Satija, S. K.; Majkrzak, C. F. *Langmuir* **1993**, *9*, 2404.

(24) McDermott, D. C.; McCarney, J.; Thomas, R. K.; Rennie, A. R. *J. Colloid Interface Sci.* **1994**, *162*, 304.

(25) Reini, H.; Brumm, T.; Bayerl, T. M. *Biophys. J.* **1992**, *61*, 1025.

(26) Schmidt, A.; Spinke, J.; Bayerl, T.; Sackmann, E.; Knoll, W. *Biophys. J.* **1992**, *63*, 1185.

(27) Krueger, S.; Ankner, J. F.; Satija, S. K.; Majkrzak, C. F.; Gurley, D.; Colombini, M. *Langmuir* **1995**, *11*, 3218.

(28) Majkrzak, C. F. *Phys. B* **1991**, *173*, 75.

sample size and are always given on a logarithmic scale. The attenuation of the neutron beam due to absorption and incoherent scattering on passing through the interface region was assessed on the basis of the corresponding neutron cross sections of the isotopes involved. This correction turned out to be crucial for the water gap between the two lipid-covered surfaces due to its comparably large thickness.

Reflectivity data were fit on the basis of model neutron scattering length density profiles. It is necessary to explicitly take into account the bilayer-coated surfaces of both silicon blocks as well as the water gap between them. This was accomplished by assuming a mirror symmetrical relationship between the scattering density profiles of the two bilayer-coated solid/aqueous interfaces.

(i) *Parametric B-Spline Profiles.* Candidate scattering length density profiles are composed of randomly generated smooth functions represented by parametric B-splines (PBS).²⁹ Three geometrical constraints are applied during each single fit. The extension of the model profile perpendicular to the substrate/subphase interface d_{tot} is kept constant. The scattering length density values on both ends of the model profiles are required to match the bulk values of the substrate (for $z \leq 0$) and of the subphase (for $z \geq d_{\text{tot}}$). Starting from an otherwise randomly chosen PBS curve, a fitting strategy is applied to discover PBS curves that reproduce the given reflectivity data. For each sample we generated a large number of model profiles with d_{tot} ranging from 60 to 85 Å with an increment of 5 Å. The density profiles $\rho(z)$ were visually screened for unphysical candidates both during and after completion of the fitting process. Profiles containing loops or backward bows in the (z, ρ) plane or regions with scattering density values considerably outside the range expected on the basis of the isotopic composition of the interface layer were abandoned.

(ii) *Stepped Function Profiles.* Starting from the general features of the neutron scattering length density profile of the interface region obtained by employing the PBS approach, a parametrized model of the interface was used. Stepped functions served as candidate profiles.³⁰ The width and the height of a box in these profiles correspond to the thickness and mean neutron scattering length density of a layer, respectively.

Atomic Force Microscopy. Small-size single-crystal silicon wafers ($12 \times 12 \times 3$ mm³) were provided by Semiconductor Processing, Inc. (Boston, MA). The surface-polishing procedure done by the manufacturer was exactly the same as for the larger blocks used for the reflectometry measurements. Cleaning of the wafers as well as preparation of a lipid layer on the surface of the wafers was done in close analogy to the neutron experiments. The adsorption of the lipid DPPC onto the wafers was performed at 55 °C. The wafers were rinsed with deionized water once at 55 °C and three times at ambient temperature. Imaging was done at room temperature with the surface of the wafer remaining immersed in water throughout the experiment. The fully hydrated lipid was in the gel phase during the experiment.

The atomic force microscope (AFM) used was a NanoScope II (Digital Instruments, Santa Barbara, CA). It was operated with an A-type scanner head (maximum scan size $1 \times 1 \mu\text{m}^2$) and a glass cantilever mount. Even though no O-ring was inserted between the cantilever mount and the wafer, the tiny gap between both surfaces remained filled with water for several hours. A V-shaped 200 μm Standard Silicon Nitride cantilever (nominal spring constant of 0.06 N/m) with a pyramidal tip at the end was used. Forces were in the range of 10^{-9} N. Scanning speed was between 3 and 10 Hz.

Results and Discussion

Adsorption of Bilayers. The kinetics of lipid adsorption at the solid/water interface were studied in SMW using the lipid DPPC- d_{62} with perdeuterated acyl chains. Although the neutron scattering length density values of silicon and SMW are identical, the bare single-crystal silicon surface exposed to SMW gives rise to a small but non-zero intensity of specular reflected neutrons. This is

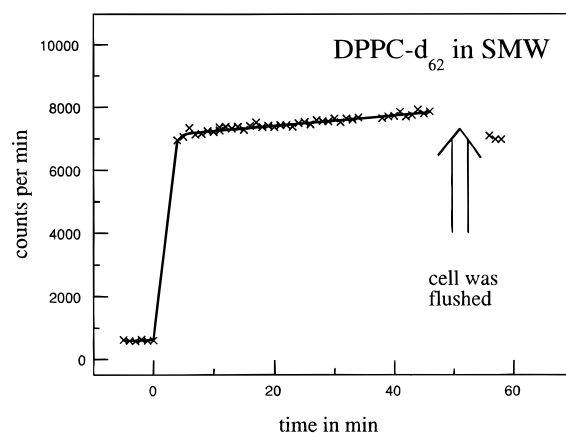


Figure 2. Kinetics of the spontaneous adsorption of small unilamellar DPPC- d_{62} vesicles at the silicon/water interface. Shown is the intensity of the reflected neutron beam at $Q = 0.009 \text{ \AA}^{-1}$. At $t = 0$ the lipid solution was poured into the sample cell; at $t = 48$ min the buffer was exchanged twice. The experiment was performed by using silicon-matched water at 60 °C. The solid line was added for clarity only.

due to the presence of a thin SiO_2 layer at that interface.³¹ However, the adsorption of deuterated material with a scattering density much higher than that of silicon to an initially bare silicon/water interface is expected to result in a large increase in intensity of the reflected neutron beam.

The lipid build-up at the interface was monitored by recording the reflected intensity at $Q = 0.009 \text{ \AA}^{-1}$ as a function of time (Figure 2). A strongly increased intensity was observed after adding a solution of small unilamellar DPPC- d_{62} vesicles into the sample cell and mixing the cell content. Although the count rate kept rising after the initial jump, the slope was much lower afterward. Rinsing the cell with pure SMW resulted in a decrease of the intensity with a final value resembling the level observed immediately after the initial jump. The observed behavior implies a very rapid build-up of a primary lipid layer at the interface, most probably a bilayer, within the first 3 min. The subsequent increase of reflected intensity indicates further adsorption of lipid at the interface, either as additional bilayer patches atop the primary layer or as loosely attached vesicles. Apparently most of the lipid adsorbed in the second step gets washed off by exchanging the buffer solution.

It is noteworthy that the reflected intensity measured at $Q = 0.009 \text{ \AA}^{-1}$ increased by about a factor of 2 after the second silicon block had been moved to within a few micrometers of the stationary block (cf. Figure 1). This hints at a comparable lipid coverage of both silicon/water interfaces and demonstrates the need to take into account both surfaces during the data processing.

Lateral Homogeneity of the Lipid Layer. AFM was used to estimate the degree of coverage of the surface of silicon wafers with a lipid bilayer and to characterize the defects of the bilayer. The force applied to the surface during scanning was sufficiently low to enable imaging of the surface topology of the lipid layer in the gel state. This was checked by intentionally damaging part of the lipid layer by increasing the imaging force. For example, square-shaped defects could be created by repeatedly scanning a fraction of the maximum accessible scan area with excessive force at a high rate (30 Hz). The boundaries of such defects could be stably imaged after readjusting the scanning force to its minimum value and increasing the scan size.

(29) Berk, N. F.; Majkrzak, C. F. *Phys. Rev. B* **1995**, *51*, 11296.

(30) Lekner J. *Theory of reflection*; Martinus Nijhoff: Dordrecht, 1987.

(31) Grunthaner, F. J.; Grunthaner, P. J. *Mater. Sci. Rep.* **1986**, *1*, 65.

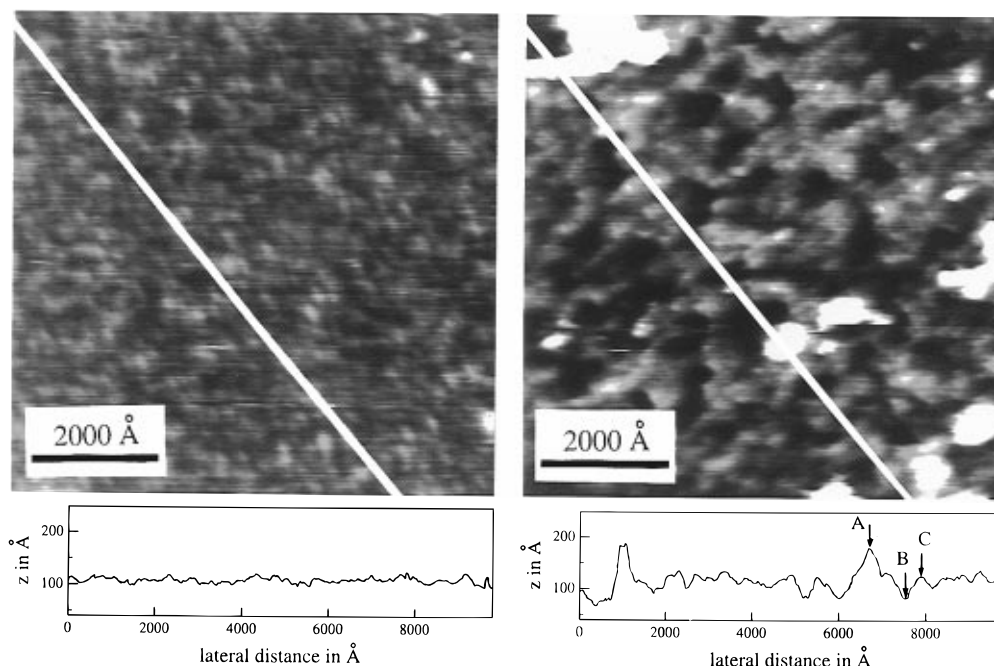


Figure 3. AFM images of a clean silicon wafer (left) and a DPPC layer adsorbed to a silicon wafer (right). Both surfaces were imaged under water at 22 °C. Depth profiles corresponding to the sections indicated with white lines are shown underneath the images. In the depth profile on the right the vertical distance between points A (two bilayers) and B (uncovered surface) is 95 Å. The distance between points B and C (single bilayer) is 43 Å.

In Figure 3 typical AFM images of a clean silicon wafer (left) and of a lipid layer adsorbed to the surface of a wafer (right) are shown. The surface of the clean wafer appears to be comparably flat and quite featureless. The height fluctuation over the entire image is of the order of ± 10 Å, and the standard deviation was determined to be 6 Å. In the case of a lipid coated wafer, basically three height levels can be distinguished. The gray-shaded areas in the top view of that surface (Figure 3, right) occupy the largest fraction of the image ($\approx 60\%$). The gray area is interrupted by black spots with typical lateral dimensions of 100–500 Å. The black spots account for about 30% of the total area and lie 40–50 Å lower than the gray-shaded areas. In addition there are a few white patches in the image (about 10% of the total area), which correspond to a height level of 40–50 Å above the gray-shaded areas. The implication is that the gray areas represent a single lipid bilayer adsorbed to the silicon surface, the black spots indicate holes in the bilayer, and the white patches are due to the presence of two bilayers. Besides the white and black patches, there seems to be an inherent roughness of the single lipid bilayer covered areas. This is attributed to both the finite roughness of the underlying surface of the wafer and the preparation of the bilayer by collapsing small unilamellar lipid vesicles at the surface of the wafer. The spontaneous adsorption technique used to coat silicon wafers with a lipid bilayer yielded a coverage of typically $70 \pm 20\%$. Defects due to holes in the SSLB were found to be uniformly distributed across the surface of the wafer.

A second scanning head was used to image larger portions of the wafer surface (maximum scan size $16 \times 16 \mu\text{m}^2$) in order to screen the lipid bilayer for larger defects. No evidence for the existence of larger defects was obtained.

Reflectivity Curves. The reflectivity curves of SSLB in $^2\text{H}_2\text{O}$ show a plateau region at very low values of Q due to total reflection of the neutron beam (Figures 5 and 6) which is absent in the measurements with SMW as subphase (Figure 4). This is expected on the basis of the corresponding neutron scattering length density values of silicon and $^2\text{H}_2\text{O}$ vs SMW as subphase.³⁰ Beyond the

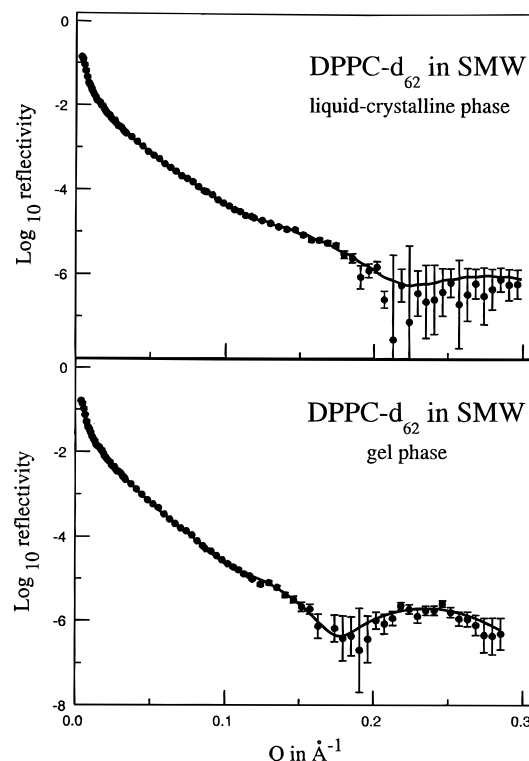


Figure 4. Neutron reflectivity curves obtained from supported single DPPC- d_{62} bilayers in silicon-matched water at 60 °C (above) and at 20 °C (below). The solid curves represent the best fits of the data achieved by using a stepped function to model the scattering density profile.

critical glancing angle for total reflection, the measured intensity drops rapidly. The counting time per data point was varied from seconds at very low Q to half an hour at $Q = 0.3 \text{ Å}^{-1}$ in order to achieve reasonable counting statistics resulting in a typical data accumulation time of 15 h per curve.

The design of the sample cell and, in particular, the introduction of the second silicon interface (Figure 1)

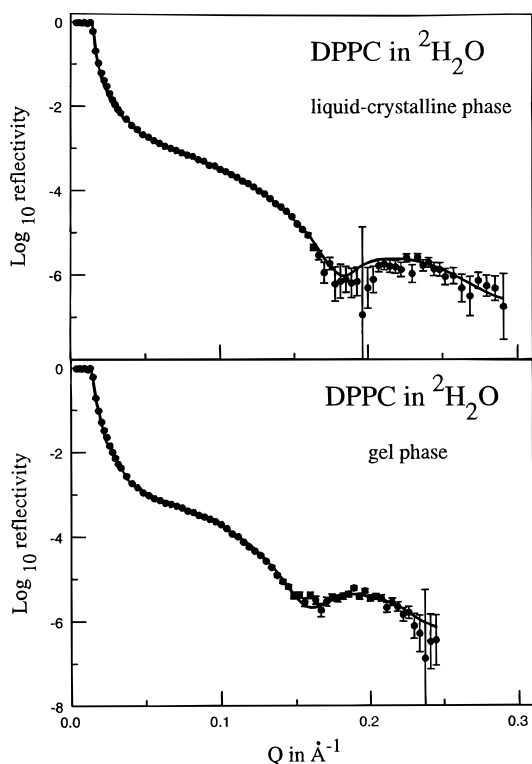


Figure 5. Neutron reflectivity curves obtained from supported single DPPC bilayers in $^2\text{H}_2\text{O}$ at 60 °C (above) and at 20 °C (below). The solid curves represent the best fits of the data achieved by using a stepped function to model the scattering density profile.

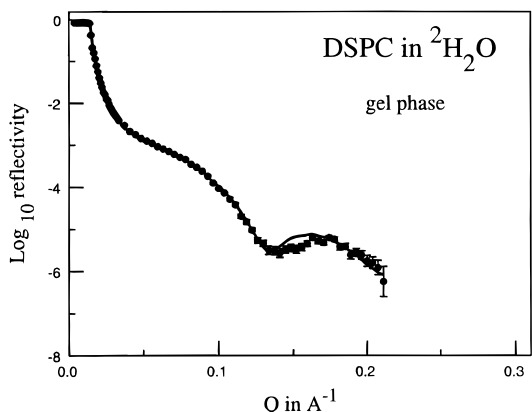


Figure 6. Neutron reflectivity curve obtained from supported single DSPC bilayers in $^2\text{H}_2\text{O}$ at 30 °C. The solid curve represents the best fits of the data achieved by using a stepped function to model the scattering density profile.

resulted in a dramatic decrease of the incoherent scattering from the subphase. The overall background level was found to be well below 10^{-6} of the intensity of the incident beam (Figures 4–6) which compares favorably with background levels above 10^{-5} reported in previous studies.^{4,26} This improvement is essential for observing the first minimum in all reflectivity curves. The position of the minimum is very sensitive to the thickness and scattering length density of the interface layer located between the single-crystal silicon substrate and the aqueous subphase. It is expected to shift towards lower Q values if the thickness of that layer increases.³⁰ This is exactly what was observed. Lowering the temperature of the DPPC bilayer from 60 to 20 °C causes the transition from the liquid-crystalline to the gel phase.³² This phase transition results in an increase in membrane thickness as seen by the shift of the position of the first minimum

in Figures 4 and 5. The larger thickness of a DSPC bilayer compared to that of a DPPC bilayer in the gel phase (Figures 5 and 6) is correctly reflected as well.

A more detailed picture of the bilayer structure can be gained from the scattering length density profiles of the interfacial layer $\rho(z)$ which are derived from the data. The two major obstacles in determining $\rho(z)$ are the non-uniqueness and the restricted resolution of the reflectivity curves. In general the density profiles which reproduce the experimental reflectivity data can be grouped in classes of profile shapes in which the members of a given class share general features but differ somewhat in the details of the structure. Choosing model profiles out of a function space such as the space of parametric B-splines has the advantage of covering practically every scattering length density profile. Therefore it is suited to deal with the nonuniqueness of reflectivity data. In contrast, a parametrized model such as a stepped function is explicitly confined to a certain model of the interface; however it allows us to quantify the structure.

The canonical resolution of the model profiles is $2\pi/Q_{\text{max}}$, where Q_{max} limits the Q range in which data other than background can be collected. Thus the successful extension of the Q range up to $Q = 0.3 \text{ \AA}^{-1}$ achieved has been crucial for improvement of the resolution of the structure of SSLB.

Parametric B-Spline Profiles. In the case of a DPPC-coated silicon wafer, the total thickness of the interface region d_{tot} between the single-crystalline silicon substrate and the aqueous subphase was found to be $70 \pm 5 \text{ \AA}$ in the gel phase and $65 \pm 5 \text{ \AA}$ in the liquid-crystalline phase. For DSPC in the gel phase a value of $80 \pm 5 \text{ \AA}$ was estimated.

For DPPC- d_{62} in SMW, both in the gel and in the liquid-crystalline phase, the density profiles discovered could be grouped in two classes of profile shapes which are mirror-symmetrical to each other, i.e. $\rho_2(z) = \rho_1(d_{\text{tot}} - z)$. This is due to the identical scattering length density of substrate and subphase. In the case of DPPC in $^2\text{H}_2\text{O}$, two classes of profile shapes occurred as well. However, these classes are related to each other by an inversion, i.e. $\rho_2(z) = 2\rho_m - \rho(d_{\text{tot}} - z)$, where $\rho_m = (\rho(0) + \rho(d_{\text{tot}}))/2$. This type of symmetry only applies if the scattering length density close to the center of the film is approximately ρ_m .

In both cases it was possible to discern the class of profile shapes which represents the structure of the interface of the sample from the other class which is mathematically correct but does not resemble the real structure. This was accomplished by assuming an identical structure of the interface region for both DPPC in $^2\text{H}_2\text{O}$ and DPPC- d_{62} in SMW and taking advantage of the large contrast in the scattering length density of the acyl chains of the lipid (cf. Table 2).

A variety of PBS profiles for both DPPC in $^2\text{H}_2\text{O}$ (above) and DPPC- d_{62} in SMW (below) in the gel phase with $d_{\text{tot}} = 70 \text{ \AA}$ is shown in Figure 7. The density profiles show a steep slope for both contrasts next to the edge of the single-crystalline silicon substrate ($z = 0$). This most likely indicates the presence of an SiO_2 layer above the substrate. A single-crystalline silicon surface is prone to spontaneous oxidation resulting in an SiO_2 coverage with a thickness in the nanometer range, depending on the environmental conditions and the treatment of the crystal.³¹ The profiles obtained with SMW as subphase show a maximum slightly below $z = 10 \text{ \AA}$ followed by a minimum slightly above $z = 15 \text{ \AA}$; however in the case of $^2\text{H}_2\text{O}$ as subphase the profiles continuously rise up to $z = 17 \text{ \AA}$. These features

(32) Cevc, G. In *Phospholipids Handbook*; Cevc, G., Ed.; Marcel Dekker: New York, 1993; p 939.

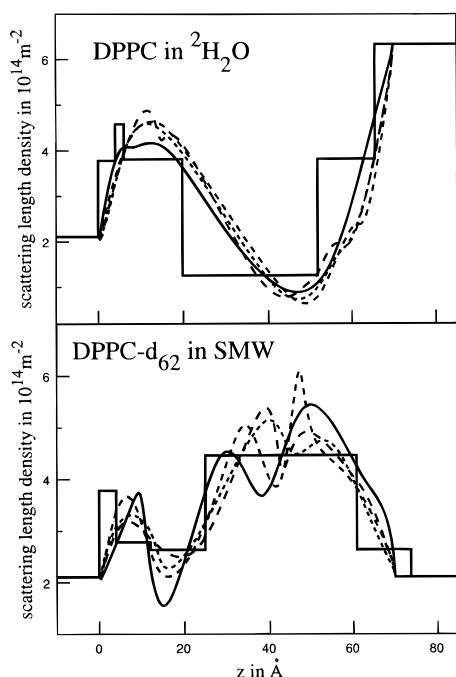


Figure 7. Neutron scattering length density profiles of DPPC normal to the lipid bilayer coated silicon/water interface. The scattering length density at $z < 0$ corresponds to the single-crystalline silicon substrate, while the plateau value on the right side symbolizes the subphase. The profiles were derived from the reflectivity curves recorded at 20 °C. The selected stepped profiles shown give the lowest χ^2 values between model and experimental reflectivity curves. The smooth PBS profiles correspond to a total interface thickness of $d_{\text{tot}} = 70$ Å and reproduce the measured reflectivity curves equally well.

are evidence for the presence of a water-rich region above the SiO_2 layer, which might be partially interpenetrated by SiO_2 spikes and/or lipid head groups. The remaining part of the profile is dominated by the lipid. The geometrical dimensions as well as the qualitative features of the scattering length density profile clearly indicate the presence of a single bilayer. The perdeuterated acyl chains of DPPC- d_{62} result in a broad maximum, while a deep trough is found at the same location for protonated DPPC. The hydrated head groups of the lipid are accommodated in the extended transition regions between the hydrocarbon core of the bilayer and the aqueous environment on both sides.

Using the PBS approach we were able to demonstrate that the lipid forms a single bilayer at the silicon/aqueous interface. Furthermore, common features of the structure of a SSLB adsorbed to that interface were determined. The thickness of the natural SiO_2 layer above the single-crystal silicon was between 5 and 10 Å. The transition between single-crystal silicon and the SiO_2 layer is not sharp but rather gradual, indicating locally varying penetration depth of SiO_2 . There was always a water-rich layer of 5–10 Å thickness between the SiO_2 layer and the lipid bilayer. The transition from SiO_2 to the water-rich region was gradual too, probably due to a jagged appearance of the SiO_2 surface. The scattering density of the bilayer itself was found to be intermediate between the theoretical values for a nonhydrated membrane (Table 2) and that for the aqueous subphase. Both hydration of the membrane and incomplete coverage of the interface with a SSLB are likely to contribute to this effect.

Comparison of the PBS profiles generated by starting from the same reflectivity curve reveals very nicely the resolution limit of the experimental data (cf. Figure 7). Obviously one has to be very careful not to overinterpret certain details of the PBS profiles. For instance, there

seems to exist an asymmetry between both leaflets of the bilayer. However, the present experimental resolution does not allow a localization or further characterization of that asymmetry.

Stepped Function Profiles. The bilayer could not be modeled as a single layer with homogeneous scattering properties. Instead a three-step profile is appropriate. It consists of a central membrane layer (CML) and two identical interface membrane layers (IML) on both sides of the CML. Thus two thicknesses and two mean scattering length density values are required to describe the bilayer. In addition, it is necessary to include two more steps representing the natural SiO_2 layer ($\rho = 3.78 \times 10^{14} \text{ m}^{-2}$) above the silicon single crystal and the water-rich transition layer between the SiO_2 and the bilayer. The thickness of the water gap between the two bilayer-covered silicon blocks brings the number of adjustable parameters to the final value of eight.

The eight-dimensional parameter space was systematically explored starting with a coarse grid size. The choice of initial parameter sets was guided by the PBS profiles. The Parrat method³³ was applied to calculate the reflectivity curve corresponding to each point of the grid taking also into account the geometry of the reflectivity experiment (computer program TMLAYER). The root mean square deviation χ^2 between calculated and experimental reflectivity curves was determined. In the vicinity of local minima of χ^2 the grid size was decreased until the minimum was sufficiently localized.

The model parameters are mutually dependent. This results in quite shallow global minima of χ^2 for all SSLB's studied and gives rise to appreciable errors of the individual parameter values (Table 1). The thickness of the central membrane layer d_{CML} as well as that of the interface membrane layer d_{IML} of DPPC are significantly larger in the gel phase than in the L_α phase. A further increase is observed for DSPC in the gel phase.

The thickness of the SiO_2 layer was 4 ± 2 Å and that of the adjacent rough SiO_2 /water layer was between 2 and 8 Å. The water gap thickness between the silicon blocks was close to 1.5 μm in all but two experiments, where a value of 12 μm was inferred.

Geometrical Fit Parameter vs Bilayer Structure.

The mean scattering length density values of the molecular subunits of the polar headgroup region of phosphatidylcholine lipids (choline, phosphate, glycerol, and carbonyl fragments) show a broad distribution.³⁴ However, the average value for the headgroup is very different from that of the fairly homogeneous hydrocarbon region (Table 2). The carbonyl fragments which are located immediately next to the hydrocarbon core have the highest scattering length density in the headgroup region. Lipids hydrogenated at their acyl chains show a quite steep jump between both regions in the scattering density profile. In a lipid bilayer deuterated at the acyl chains, the scattering length density of the fatty acid chains is much higher than that of the polar region (Table 2). We conclude that the central membrane layer (CML) and the interface membrane layer (IML) used to describe the bilayer in the stepped function model correspond in a first approximation to the hydrocarbon core and the polar headgroup region of the bilayer. Nevertheless, owing to the detailed scattering density profile, there might be slight differences in the bilayer regions physically represented by the CML and the IML in the case of a hydrogenated lipid in $^2\text{H}_2\text{O}$ and a fatty acid deuterated lipid in SMW.

Thickness Values. X-ray diffraction measurements on fully hydrated DPPC multilamellar membrane stacks

(33) Parratt, L. G. *Phys. Rev.* **1954**, *95*, 359.

(34) Wiener, M. C.; White, S. H. *Biophys. J.* **1992**, *61*, 434.

Table 1. Stepped Function Model Parameters^a Describing the Bilayer

sample	temp (°C)	d_{CML} (Å)	d_{IML} (Å)	ρ_{CML} ($\times 10^{14} \text{ m}^{-2}$)	ρ_{IML} ($\times 10^{14} \text{ m}^{-2}$)
DPPC in $^2\text{H}_2\text{O}$	20	32 ± 2	13.7 ± 0.8	1.26 ± 0.05	3.9 ± 0.1
	60	28 ± 2	11.5 ± 1.0	-0.12 ± 0.05	3.4 ± 0.1
DPPC- d_{62} in SMW	20	36 ± 2	15.5 ± 2.5	4.57 ± 0.2	2.6 ± 0.2
	60	29 ± 2	13 ± 3	4.97 ± 0.2	2.7 ± 0.2
DSPC in $^2\text{H}_2\text{O}$	30	38 ± 2	16 ± 1	1.25 ± 0.05	3.7 ± 0.1

^a Abbreviations: d_{CML} , thickness of the central membrane layer; d_{IML} , thickness of the interface membrane layer; ρ_{CML} , mean neutron scattering length density of the central membrane layer; ρ_{IML} , mean neutron scattering length density of the interface membrane layer.

Table 2. Selected Molecular Volumes v and Neutron Scattering Length Density Values ρ for $\lambda = 2.367 \text{ Å}$

	v (Å ³)	ρ ($\times 10^{14} \text{ m}^{-2}$)
DPPC polar head group region	348	1.73
DPPC hydrocarbon region at 20 °C	790	-0.41
DPPC hydrocarbon region at 60 °C	896	-0.36
DPPC- d_{62} hydrocarbon region at 20 °C	790	7.74
DPPC- d_{62} hydrocarbon region at 60 °C	896	6.82
single-crystal silicon		2.11
SiO ₂		3.78
silicon-matched water	30	2.11
$^2\text{H}_2\text{O}$	30	6.38

at 20 °C gave a thickness of the hydrocarbon region of $35 \pm 1 \text{ Å}$.³⁵ In the L_α phase a value of 26 Å was reported for large unilamellar DPPC vesicles.² In addition, one can estimate the thickness of the hydrocarbon region of DSPC in the gel phase to be $38.6 \pm 1 \text{ Å}$ by starting from the known value for DPPC ($35 \pm 1 \text{ Å}$), assuming a length increment along the chain of 1.27 Å per additional methylene segment and using the known tilt angles of the acyl chains of DPPC (32°) and DSPC (33.5°).³⁶ These numbers coincide in the limits of experimental error with the d_{CML} values obtained here for the corresponding supported single lipid bilayers (cf. Table 1), indicating the absence of changes of the thickness of the hydrophobic core of the bilayer due to the presence of the solid support.

It is difficult to relate the parameter d_{IML} to a structural entity determined in multilayer measurements. Hydration of the head groups, surface roughness, and the highly dynamic state of the bilayer cause a very gradual transition of the scattering length density between the headgroup of the membrane and the adjacent water subphase. Moreover, the similarity of the mean scattering length density of the lipid head group region and of SMW (cf. Table 2) results in an increased uncertainty of the parameters d_{IML} and ρ_{IML} for these cases. In a very coarse approximation one can relate d_{IML} to half the difference between the multilayer repeat spacing and the hydrocarbon core thickness. On the basis of the diffraction data published by Wiener et al.³⁵ for DPPC multilayers at 20 °C, this quantity amounts to $14.4 \pm 0.5 \text{ Å}$. This compares well with our values of d_{IML} for supported single DPPC bilayers at 20 °C. The $d_{\text{IML}} = 16 \pm 1 \text{ Å}$ determined for DSPC seems to be a little high since no difference in the head group structure of multilamellar DPPC and DSPC has been detected so far.³⁶

Area per DPPC Molecule. On the basis of the density measurements of Nagle and Wilkinson³⁷ we have calculated the volumes of the DPPC polar regions (all of the lipid molecule but the hydrocarbon chains) and of its hydrocarbon region (Table 2). Note the temperature dependency of the volume of the latter. The values do not include any waters of hydration. We assumed the molecular volumes not to change upon deuteration.

Both the decrease of the volume of the hydrocarbon region and the increase of its thickness during the transition from the L_α to the gel phase contribute to a decrease of the area, A , per lipid molecule in a plane perpendicular to the bilayer normal. The difference in hydrocarbon core thickness determined for DPPC translates into an area change of about 25% if one assumes that no water or void volume is present in the hydrocarbon region and that the area per molecule in the L_α phase is about 65 Å^2 .³⁸ Since the volume of the polar head group of the lipid remains nearly constant over the temperature range studied,³⁷ one would expect a thinning of the head group region upon increase of the temperature from 20 to 60 °C. Indeed, the parameter d_{IML} of DPPC in the L_α phase appears to be smaller (Table 1). A quantitative comparison is difficult since the hydration level of the head group might change as well.

Bilayer Coverage of the Substrate. The fitted scattering length density values ρ_{CML} and ρ_{IML} (Table 1) are different from the mean values calculated for non-hydrated hydrocarbon core and polar head group region of DPPC (Table 2). The values obtained for DPPC- d_{62} in SMW are too far off to be accounted for by direct hydration of the individual lipid molecules. The most likely explanation is an incomplete coverage of the surface of the wafer with a lipid bilayer. The spontaneous adsorption of small unilamellar lipid vesicles at the interface during the coating process probably results in bilayer patches containing the lipid molecules of individual collapsed vesicles in alternation with noncovered areas. The final coverage depends on the exact regime of the coating process as well as on the surface properties of the substrate. The average size of the covered regions as well as that of the uncovered regions is crucial for the data treatment. If the lateral extension of the domains of either kind is small compared to the coherence length of the neutrons (10–100 μm at least), the reflectivity experiment simply averages over the scattering length values in a given layer parallel to the interface. In this case one could use the experimentally obtained scattering length density values to estimate the coverage of the surface with a bilayer. However, if the dimension of either the uncovered or the bilayer-coated domains were to exceed the coherence length of the neutrons, then the observed reflectivity curve would be a superposition of individual reflectivity curves from qualitatively different regions including cross terms.

The additional experiments performed by using AFM clearly indicate that the lateral dimensions of uninterrupted patches of both kinds are well below the coherence length of the neutrons. Consequently, it is correct to assume that the fitted scattering length density values ρ_{CML} are an average over pure hydrocarbon layer in the membrane patches and water layer in the uncovered regions. For DPPC in $^2\text{H}_2\text{O}$ we obtained values of the hydrocarbon content of $93 \pm 1 \text{ vol } \%$ at 60 °C and $75 \pm 1 \text{ vol } \%$ at 20 °C. The corresponding figures for DPPC- d_{62}

(35) Wiener, M. C.; Suter, R. M.; Nagle, J. F. *Biophys. J.* **1989**, *55*, 315.

(36) Tristram-Nagle, S.; Zhang, R.; Suter, R. M.; Worthington, C. R.; Sun, W.-J.; Nagle, J. F. *Biophys. J.* **1993**, *64*, 1097.

(37) Nagle, J. F.; Wilkinson, D. A. *Biophys. J.* **1978**, *23*, 159.

(38) Seddon, J. M. In *Phospholipids Handbook*; Cevc, G., Ed.; Marcel Dekker: New York, 1993; p 909.

in SMW are 61 ± 4 vol % at 60 °C and 44 ± 3 vol % at 20 °C. The value for DSPC in $^2\text{H}_2\text{O}$ at 30 °C is 76 ± 1 vol %. These figures can be interpreted as a coarse measure of the coverage of the silicon surface with a lipid bilayer and are in agreement with the AFM data, which indicate a coverage of $70 \pm 20\%$ for DPPC in the gel phase.

The coating of the silicon substrate with a bilayer was always done with lipids in the L_α phase. After completion of the coating process and removal of excess lipid from solution the amount of lipid at the silicon surface cannot increase. The most likely reason for the strong decrease of the covered surface area by 18% (DPPC in $^2\text{H}_2\text{O}$) and 17% (DPPC- d_{62} in SMW) upon lowering the temperature from 60 °C to 20 °C is the decrease of the lipid molecular area perpendicular to the membrane normal. Our data indicate a shrinkage of the size of the membrane patches and/or a further fragmentation of the bilayer covered areas at the silicon/water interface in favor of uncovered regions upon decrease of the temperature. Bearing in mind the shortcomings of the stepped function as a model of a membrane, the calculated decrease of surface coverage is fairly close to the expected relative decrease of the area per DPPC molecule of 25% over the temperature range studied.

The hydrocarbon content of 93 vol % for DPPC in $^2\text{H}_2\text{O}$ in the L_α phase indicates a nearly complete coverage of the solid/water interface with a single lipid bilayer. The much lower coverage (61%) achieved with DPPC- d_{62} in SMW under the same conditions is most likely the result of the deterioration of the surface properties of the single-crystal silicon blocks after several experiments. The measurements with DPPC in $^2\text{H}_2\text{O}$ were done after the replacement of the blocks and the obtained coverage seems to be close to that in the earlier experiment with DSPC in $^2\text{H}_2\text{O}$. The lower coverage of the silicon blocks in the SMW experiments may be accompanied by an increased size of patches of uncovered areas. This patch size may approach the coherence length of the neutrons. In order to estimate the influence of such a behavior on the fit parameters we calculated a theoretical reflectivity curve in the range $0 \leq Q \leq 0.3 \text{ \AA}^{-1}$ for the extreme case of half of the silicon/water interface covered with a bilayer and the other half uncovered. The thickness parameters obtained by fitting this theoretical curve are very close to the values used to mimic the bilayer covered part of the interface. However, the fitted scattering length density values deviated by more than 10% from that of a uniform layer consisting of small-size lipid and water patches. The implication is that even for domain sizes well above the coherence length of the neutrons, the fitted thickness parameters perhaps do still reasonably reflect the interface structure while the scattering length density values do not. This is in agreement with the proximity of the thickness parameters obtained from the measurements on DPPC in $^2\text{H}_2\text{O}$ and DPPC- d_{62} in SMW despite the quite different levels of surface coverage.

The estimation of the surface coverage from the fitted scattering length density values of the interface membrane layer is prone to artifacts. The polar head group region of the bilayer is expected to contain some water of hydration. A constant scattering length density across the head group region is a very simplified model of that region and represents an average of static and dynamic fluctuations of the location of the lipid molecules perpendicular to the substrate surface. These shortcomings are most obvious in the ρ_{IML} values obtained for DPPC- d_{62}

in SMW. In the frame of the model they are expected to lie between the scattering length density values of the nonhydrated polar region of the bilayer and of SMW. However, they were found to be outside this range (Table 1).

Silicon Oxide/Water Layer. The total thickness of the SiO_2 layer above the single-crystal silicon including a jagged surface layer containing some water and perhaps the outermost fraction of the lipid headgroups was estimated to be 6–12 Å based on the fits using the stepped function profiles. The PBS fits seem to favor a slightly higher value of about 15 Å (cf. Figure 7). Even though a precise description of the structure of this region is beyond the scope of the resolution of the present reflectivity curves, the cited values are significantly smaller than the 30 ± 10 Å determined by Johnson et al.⁴ for the thickness of an intermediate jagged quartz/water layer between a quartz substrate and a supported single DMPC bilayer. This might be related to the higher mechanical stability of SSLB on single-crystal silicon substrates as compared to quartz as reported in the literature.^{13,39}

Summary

The previously determined structure of the DPPC bilayer in the multilamellar state is fairly well conserved at the surface of a silicon substrate. Despite the support of the bilayer by a solid surface, only minor changes in the physical properties of the bilayer have been reported in the literature.^{9,13} One side of the single lipid bilayer has access to the bulk water phase. This makes the SSLB a superior model system for studying structural aspects of biologically relevant membrane interactions as compared to more common multilamellar systems.

Although the reflectivity experiment requires a large surface to be coated with the bilayer, the actual amount of lipid forming the bilayer is not more than 0.1 mg. Moreover, even though we performed experiments with both deuterated and protonated lipids, the data processing was done independently for both cases. Thus the structural resolution achieved here for protonated lipids in $^2\text{H}_2\text{O}$ should apply also for SSLB reconstituted from naturally occurring membrane components without the need to use isotopically labeled substitutes.

By combining neutron reflectivity measurements and atomic force microscopy it was possible to gain insight in both the vertical as well as the lateral structure of solid supported single lipid bilayers in an aqueous environment.

Acknowledgment. We thank Dr. J. F. Ankner (University of Missouri) for providing the program TMLAYER. Helpful discussions with C. Naumann (Technische Universität München) in the very early stages of this work as well as with Dr. L. Tamm (University of Virginia) are gratefully acknowledged. B.W.K. was financially supported by a postdoctoral fellowship from the German Academic Exchange Service. S.K., W.J.O., and C.F.M. were partly supported by the National Science Foundation under Agreement No. DMR-9122444.

LA950580R

(39) Bayerl, T. M.; Bloom, M. *Biophys. J.* **1990**, *58*, 357.

(40) Certain commercial material and equipment are identified in this paper in order to specify experimental procedures. This in no way implies recommendation or endorsement by the National Institute of Standards and Technology.